Received: 13 April 2021 | Revised: 15 July 2021 | Accepted: 15 July 2021

DOI: 10.1111/pce.14226

ORIGINAL ARTICLE

Plant, Cell & Environment | WILEY

Alpine dwarf shrubs show high proportions of nonfunctional xylem: Visualization and quantification of species-specific patterns

Andrea Ganthaler[1] | Andreas Bär[1] | Birgit Dämon[1] | Adriano Losso[1,2] | Andrea Nardini[3] | Christian Dullin[4,5,6,7] | Giuliana Tromba[4] | Georg von Arx[8] | Stefan Mayr[1]

[1]Department of Botany, University of Innsbruck, Innsbruck, Austria

[2]Hawkesbury Institute for the Environment, Western Sydney University, Richmond, New South Wales, Australia

[3]Dipartimento di Scienze della Vita, Università di Trieste, Trieste, Italy

[4]Elettra-Sincrotrone Trieste, Basovizza, Italy

[5]Institute for Diagnostic and Interventional Radiology, University Medical Center, Göttingen, Germany

[6]Max-Planck-Institute for Experimental Medicine, Göttingen, Germany

[7]Diagnostic and Interventional Radiology, University Hospital, Heidelberg, Germany

[8]Swiss Federal Institute for Forest, Snow and Landscape Research WSL, Birmensdorf, Switzerland

Correspondence
Andrea Ganthaler, Department of Botany University of Innsbruck, Sternwartestrasse 15, 6020 Innsbruck, Austria.
Email: andrea.ganthaler@uibk.ac.at

Funding information
L'Oreal Austria fellowship, Grant/Award Number: 2016; to A. Ganthaler; Bundesministerium für Bildung, Wissenschaft und Forschung, Grant/Award Number: excellence grant 2018; to A. Ganthaler; Austrian Science Fund (FWF), Grant/Award Numbers: P29896, P32203, I4918, J4300; Elettra-Sincrotone Trieste, Grant/Award Number: 20165277

Abstract

Xylem conductive capacity is a key determinant of plant hydraulic function and intimately linked to photosynthesis and productivity, but can be impeded by temporary or permanent conduit dysfunctions. Here we show that persistent xylem dysfunctions in unstressed plants are frequent in Alpine dwarf shrubs and occur in various but species-specific cross-sectional patterns. Combined synchrotron micro-computed tomography (micro-CT) imaging, xylem staining, and flow measurements in saturated samples of six widespread Ericaceae species evidence a high proportion (19%–50%) of hydraulically nonfunctional xylem areas in the absence of drought stress, with regular distribution of dysfunctions between or within growth rings. Dysfunctions were only partly reversible and reduced the specific hydraulic conductivity to 1.38 to 3.57 $\times 10^{-4}$ m^2 s^{-1} MPa^{-1}. Decommission of inner growth rings was clearly related to stem age and a higher vulnerability to cavitation of older rings, while the high proportion of nonfunctional conduits in each annual ring needs further investigations. The lower the xylem fraction contributing to the transport function, the higher was the hydraulic efficiency of conducting xylem areas. Improved understanding of the functional lifespan of xylem elements and the prevalence and nature of dysfunctions is critical to correctly assess structure-function relationships and whole-plant hydraulic strategies.

KEYWORDS
embolism, Ericaceae, growth form, hydraulic conductivity, hydraulic dysfunction, micro-CT, nondestructive imaging, water transport, woody plants, xylem anatomy

1 | INTRODUCTION

Efficient long-distance water transport is paramount for survival and growth of land plants. Stem hydraulic conductance is a major factor limiting the capability to transport water to transpiring leaves and to replace the evaporative losses that occur while atmospheric CO_2 is diffusing through the stomata (McCulloh & Woodruff, 2012). Thus, water transport capacity is intimately linked to photosynthesis, and the maintenance of long-distance water transport is essential to plant health and productivity (Hubbard et al., 2001). The evolution of a specialized tissue, the xylem, which comprises different cell types that fulfil specific functions, enabled the development of a wide range of structural and functional and thus ecological adaptations of terrestrial plants (Pratt & Jacobsen, 2017). While gymnosperm xylem mainly consists of single-celled tracheids, angiosperm xylem became more specialized by the formation of multicellular vessels for efficient water transfer and fibres with thick cell walls for structural support (Tyree & Zimmermann, 2002). Combined with pronounced secondary stem growth, this tissue allows woody species to move water efficiently from roots to the crown, and thus from regions of high water availability to areas of low water availability within the soil-plant-atmosphere continuum (Sperry, 2003). Besides being efficient, xylem needs to withstand drought and freezing stress, which may block water transport by causing cavitation and air-filled conduits (Sperry & Sullivan, 1992; Utsumi et al., 1998).

The optimal water transport system in plants thus theoretically should maximize hydraulic conductance and at the same time minimize the risk of xylem cavitation for a given investment in transport tissue (Hubbard et al., 2001; Sperry, 2003). However, the secondary xylem of woody plants fulfils several basic functions as, apart from water transport, mechanical support of the plant body and storage of water and nutrients (Pratt & Jacobsen, 2017). Higher mechanical requirements, for example, can lead to reduced hydraulic conductivity, because plants devote a higher proportion of their cross section to mechanical function. Anatomical and physiological requirements regarding different wood functions are partially opposed to each other, consequently leading to functional trade-offs and species-specific adaptations as a function of varying environmental conditions. This applies to the proportion of cell types, but also to the expression of specific conduit and pit traits. Due to considerable differences in the wood structure and function, trade-offs may vary between gymnosperms and angiosperms (Choat & Pittermann, 2009).

Functional xylem conduits (vessels and tracheids) normally contain water and are hydraulically connected, establishing continuous water columns. The formation of embolism in xylem conduits can cause blockages and dramatically reduce the plant hydraulic capacity, as does the presence of nonconductive xylem elements in general. It is well-known that in long-living plants with extensive secondary growth, older growth rings lose their transport function as they turn into heartwood. This is an important, but yet not completely understood process during ontogenesis with considerable impact on whole-tree hydraulic efficiency (e.g., McDowell et al., 2002). The conversion of sapwood to heartwood was interpreted, for instance, as a response to the necessity of additional mechanical stability, higher wood resistance to decay, growing maintenance costs of living tissue, increasing transport distance from the phloem, and maintenance of xylem conductance at the same level with phloem conductance (Hölttä et al., 2013). Heartwood formation is usually accompanied by vessel occlusion through tyloses and gums to seal them off from functional xylem parts, whereby vessel embolism and air entrance was identified to act as a trigger for this process (De Micco et al., 2016; Tyree & Zimmermann, 2002). The functional lifespan (the period hydraulic functionality is maintained) of xylem conduits can largely vary between species but also within the stem cross section, leading to varying proportions of hydraulically nonfunctional elements (Jacobsen et al., 2007, 2018). However, there is only a rudimentary understanding of the functional status of xylem over time, the prevalence and nature of nonfunctional xylem conduits during periods without stress, and the impact of nonconductive xylem elements on plant transport capacity (compare also Brodersen et al., 2019). Quantitative assessment of their proportion in the xylem tissue is highly desirable for a better assessment of structure–function relationships, for example in allometric scaling models (Petit & Anfodillo, 2009), and a better understanding of whole-plant hydraulic strategies. This applies to all kinds of plant organs and growth forms, ranging from trees to lianas and shrubs.

Dwarf shrubs (also called 'subshrubs') are a group of woody plants with a characteristic low growth height. They represent a specific growth form and are a key component of the high elevation vegetation belt (Körner, 2003). They have a high relevance for structure and functioning of Alpine plant communities and are designated as important indicator species for environmental changes (Carrer et al., 2019; Maestre et al., 2016). Most species of Alpine dwarf shrub heaths belong to the family Ericaceae; they are creepers to upright plants of about 60 cm height and partly deciduous or evergreen (Larcher, 2003). Plants in this environment are exposed to harsh climatic conditions including low temperature, persisting snow cover, intensive radiation, and high wind load (Cernusca, 1976). However, thanks to their reduced growth height and compact growth form, dwarf shrubs strongly profit from more favourable near-surface conditions, formation of their own microclimate, and snow cover protection during winter. Although individual species frequently coexist and form dense carpets, their characteristic clustered distribution is strongly shaped by the topography and snow cover dynamics during winter (Carrer et al., 2019; Neuner, 2014). For plants in this extreme environment, it is of particular importance to balance and coordinate xylem investments between the different wood functions (see above).

While several ecological and physiological aspects of Alpine dwarf shrub heaths were intensively investigated (e.g., Grabherr, 1980; Körner, 2003; Larcher, 2003), hydraulic characteristics of this growth form are mostly overlooked. Preceding analyses on *Vaccinium* species (Ganthaler & Mayr, 2015a, 2015b) revealed both a comparably low specific hydraulic conductivity (k_s between 0.84 and 1.23×10^{-4} m^2 s^{-1} MPa^{-1}) and low resistance to drought-induced cavitation (50% loss of conductivity between −1.87 to

−2.70 MPa). Although the combination of low hydraulic safety and efficiency is not uncommon, particularly for plants of shorter stature (Bittencourt et al., 2016; Gleason et al., 2016), a large discrepancy between measured and modelled (based on conduit diameters) k_s pointed to a low proportion of conduits in the xylem and/or a high proportion of conduits that do not contribute to the transport function (Ganthaler & Mayr, 2015a). Dwarf shrubs were also chosen as study objects as they represent an important group of woody plants at high altitudes and latitudes, are adapted to high stress levels, and cover various ecological niches based on highly divergent physiological adaptations (including foliar, wood and root traits). Moreover, their low growth height enables to sample entire plants and to analyse the intact main stem, and thus to avoid cutting artefacts (Beikircher & Mayr, 2016; Sperry, 2013).

Determination of conduit functionality and detailed characterization of xylem dysfunctions is challenging and the paucity of comprehensive data sets on this topic including several species is likely due to methodological challenges. One approach comprises the staining of conducting xylem elements by perfusion of stem segments with dye and subsequent determination of the stained (=conductive) cross-sectional xylem area. This method has already been shown to be a reliable alternative or complementary method to determine the functional status of xylem elements and to quantify the percent loss of conductivity with progressive dehydration on various types of samples (Hietz et al., 2008; Jacobsen et al., 2007, 2018; Mayr & Cochard, 2003; Nolf et al., 2016; Taneda & Sperry, 2008). However, it is a destructive method and requires cutting and preparation of stem segments, with potential undesired side effects on the analyses. In contrast, X-ray micro-computed tomography (micro-CT) enables to analyse intact plants (Brodersen et al., 2019; Cochard et al., 2015). Particularly synchrotron-based micro-CT offers high spatial resolution and fast nondestructive analysis, based on rapid methodological advances in the last decade, and it has been applied successfully to assess the functional status of xylem conduits following drought and freeze-thaw stress in various species and functional plant groups (e.g., Choat et al., 2015; Knipfer et al., 2015; Losso et al., 2019; Mayr et al., 2020; Nardini et al., 2017).

Here we used micro-CT to analyse conduit functionality in hydrated (and in preceding weeks not stressed) plants and combined it with analyses based on the staining technique. From synchrotron micro-CT images, the water-filled versus gas-filled status of individual xylem conduits could be identified (see also Figure S1), and from stained samples, the proportion of stem cross section consisting of embolised tissue could be calculated. Main aims of this study were to (1) get detailed insights into the inter-specific variation in proportion and distribution of dysfunctions by comparative analysis of six co-occurring angiosperm species, (2) unravel the efficiency of water transport by distinguishing between the conductivity of entire stems and the specific hydraulic conductivity of conducting areas, and (3) analyse the relation between nonfunctional xylem areas and age of xylem tissue, metabolic status of the parenchyma, and specific xylem conductivity. Accordingly, the six dwarf shrub species *Arctostaphylos uva-ursi* (L.) Spreng., *Kalmia procumbens* (L.) Gift & Kron, *Calluna vulgaris* (L.) Hull, *Erica carnea* L., *Vaccinium myrtillus* L. and *Vaccinium gaultherioides* Bigelow (Table 1) were sampled and analysed in fully hydrated conditions by staining conductive xylem, micro-CT imaging, and hydraulic measurements, complemented by detailed image analysis. In addition, in-depth analyses on parenchyma metabolic status, vulnerability to cavitation of inner and outer growth rings and relation of nonfunctional xylem areas and hydraulic conductivity with growth ring number were performed for *A. uva-ursi*. This species was selected, as nonfunctionality was clearly related to xylem age, dysfunctions were reversible by high-pressure flushing, and stems were long enough for measurements in the centrifuge. The study should improve our knowledge of the prevalence, distribution, and nature of persistent nonfunctional xylem conduits during the growing season in plants that did not experience an extreme drought event or controlled dehydration, an important aspect for the plant hydraulic architecture.

2 | MATERIAL AND METHODS

2.1 | Study sites and plant material

The main study was conducted at two sites near Innsbruck, Austria. Samples of *E. carnea* were collected at Höttinger Bild (980 m; 47°17'N; 11°22'E; calcareous soil), all other species at Mt

TABLE 1 Characterization of analysed dwarf shrub species according to Landolt (2010), including distribution range (altitude), leaf phenology, height, soil reaction, root depth, vegetative spread (bgr, belowground runner; cs, creeping shoots) and moisture indicator number (M-No.; ranging from 1—*very dry* to 4—*wet*)

Species		Altitude	Phenology	Height (cm)	Soil reaction	Root depth (cm)	Veget.spread	M-No.
Vm	*Vaccinium myrtillus*	Montane-subalpine	Deciduous	15–50	Calcifuge	25–50	bgr	3
Vg	*Vaccinium gaultherioides*	Subalpine-alpine	Deciduous	30–60	Calcifuge	<25	bgr	3,5
Cv	*Calluna vulgaris*	Montane-subalpine	Evergreen	20–40	Calcifuge	25–50	bgr	3
Au	*Arctostaphylos uva-ursi*	Subalpine-alpine	Evergreen	5–10	Vague, silicate	50–100	cs	2
Kp	*Kalmia procumbens*	Subalpine-alpine	Evergreen	3–10	Calcifuge	<25	cs	2
Ec	*Erica carnea*	Subalpine-alpine	Evergreen	15–30	Calcicoles	25–50	cs	2

Patscherkofel (1883 m; 47°22'N, 11°47'E; siliceous soil; Table 1). To test the consistency of results across sites of varying elevation and climatic conditions, staining analyses were repeated on additional samples from Rinner Alm (1667 m; 47°13'N, 11°30'E), Serles (1695; 47°7'N, 11°24'E), Praxmar (1614 m; 47°09'N, 11°08'E) and Innsbruck Botanical Garden (615 m; 47°16'N, 11°22'E). Staining and hydraulic measurements were performed between June and August 2016, and micro-CT observations were enabled by access to the synchrotron beamline in September 2017. For all analyses, entire plants including major roots were collected after a rain period from the field sites and transported, with their roots in water and covered with a dark plastic bag, to the laboratory, where they were saturated overnight before analysis. During summer, analysed species experienced an overall favourable hydraulic situation at the study site, as stem water potentials remained above −1.4 MPa even during an intense summer drought period (Ganthaler & Mayr, 2021). Based on the vulnerability thresholds to drought-induced cavitation of these species reported in Ganthaler and Mayr (2021), we can conclude that these water potentials could not have induced significant embolization. Measurements were made on healthy plants with no visible damage (such as wilting, fungal infestation, or herbivory), whereby each analysed stem (diameter between 2.5 and 4.5 mm) originated from a different plant.

2.2 | Conductivity measurements

The flow rate was determined on 3–5 cm long fully hydrated stem sections ($n = 10$ for each species) via a modified Sperry apparatus (Sperry et al., 1988) with a mini-flow metre (mini-Cori-Flow100 g h^{-1}, Bronkhorst High Tech) at a pressure of 5 kPa using distilled, filtered (0.22 µm) and degassed water containing 0.005% Micropur (Katadyn Products) to prevent microbial growth. The specific hydraulic conductivity (k_s; m^2 s^{-1} MPa^{-1}; Sperry et al., 1988) was calculated as

$$k_s = Q \times \frac{l}{A \times \Delta P}, \quad (1)$$

where Q is the volume flow rate (m^3 s^{-1}), l is the length of the sample (m), A is the xylem cross-sectional area (m^2) and ΔP is the pressure difference between the segment ends (Pa). Calculations were corrected to 20°C to account for changes in fluid viscosity with temperature. The corrected specific hydraulic conductivity (k_{sc}) was calculated in an analogous manner, the only difference being the use of the conducting xylem cross-sectional area (A_c) instead of the entire xylem area:

$$k_{sc} = Q \times \frac{l}{A_c \times \Delta P}, \quad (2)$$

whereby A_c was determined immediately following conductivity measurements for each sample by perfusion with safranin as described in the following.

2.3 | Safranin staining

The conductive xylem area was determined by perfusing samples previously used for conductivity measurements with safranin and subsequent measurement of the entire and stained cross-sectional xylem area. Therefore, samples ($n = 10$ for each species) were sealed in a hydraulic system connected to a reservoir filled with 0.1% (w/v) filtered (0.22 µm) safranin (modified after Hietz et al., 2008 and Sperry et al., 1988). Pressure was set to 5 kPa and samples remained connected until the outflow end showed intense staining. After a drying period of 30 min at room temperature, cross sections were made from the middle part of stained stem segments with a G.S.L slide microtome (Gärtner et al., 2014) and analysed with a light microscope (Olympus BX41; Olympus Austria) interfaced with a digital camera (ProgRes CT3; Jenoptik). Pictures were evaluated with the software ImageJ (ImageJ 1.45; public domain, National Institutes of Health) using the in-built function 'colour threshold' to automatically detect stained and unstained xylem areas (after removing the pith area), and the area and distribution of conducting xylem parts were determined. Finally, the percent of conducting xylem area ($xylem_{cond}$, %) was calculated as

$$xylem_{cond} = \frac{A_c}{A} \times 100, \quad (3)$$

whereby A_c is the conducting xylem cross-sectional area (m^2) and A the entire xylem cross-sectional area (m^2). Furthermore, to test whether nonfunctional conduits were air-filled or permanently blocked, an additional stem section from the same plant and shoot was flushed three times for 20 min at 70 kPa with water to remove all potentially present embolism, and then perfused with safranin and evaluated as described above.

2.4 | Micro-CT observations

Nondestructive synchrotron-based micro-CT observations were performed on 1–2 plants per species to assess the occurrence and distribution of nonfunctional xylem conduits in intact shoots and to confirm patterns detected by safranin staining. As access to the synchrotron facility was granted subsequent to hydraulic and staining analyses, new plants of the analysed species were sampled at the study sites as described above, hydrated, and transported to the SYRMEP beamline of the Elettra Light Source in Trieste, Italy (www.elettra.trieste.it). Sample preparation and measurements followed the protocol given in Losso et al. (2019). Briefly, before measurement a 20–25 cm long main shoot of each plant was detached from the roots under water, the shoot basal end was re-cut several times, and the cut end sealed in a plastic vial containing water. The plant was stabilized with a thin woody skewer, wrapped together with the vial entirely in Parafilm® to prevent further desiccation during the scan, and fixed in a custom-made sample holder 12 cm distant from the

detector (Losso et al., 2019). This procedure allowed an easy and fast positioning of the sample and avoided long exposition to irradiation during the initial sample alignment, thus minimizing eventual X-ray induced cellular damage (Petruzzellis et al., 2018). Overall, sample preparation, initial alignment, and scan time (90 s) were performed within 10–15 min. The scanned region of the stem was about 8 cm above the root collar (corresponding to stem samples used for conductivity measurements and safranin staining), and 12 cm distant from the detector. The field of view was 5 × 5 mm and covered the entire stem diameter (see 3D reconstruction in Figure S6). Two 5 mm filters of silicon were used to obtain an average X-ray source energy of 25 keV, the exposure time was set to 100 ms, and the angular steps to 2° s^{-1}. During the 180° rotation of the sample, 900 projections were acquired.

Measurements of Ψ immediately after the scan with a portable pressure chamber (3005 Plant Water Status Console; Soil moisture Equipment Corp.) proved that plants did not dehydrate during the measurement (Ψ = 0 to −0.2 MPa). Finally, the stem (still wrapped in Parafilm®) was cut to about 1 cm length and dehydrated for at least 24 h to ensure cavitation of all conduits. Then samples were re-scanned at the marked position of the first scan to observe fully embolised xylem (Losso et al., 2019). For each sample and scan, we reconstructed 1400 slices with a pixel size of 2 µm using the software SYRMEP TomoProject (Brun et al., 2015), whereby a phase retrieval pre-processing filter (Paganin et al., 2002) was applied before using the Filtered Back Projection algorithm. The phase-retrieval enabled to obtain high-quality images and to accurately recognize water- and air-filled cells, even in these species with comparably small conduits (see also Figure S1). Then, one central slice per scan was exported as TIF file.

2.5 | Stem cross sections

Wood samples (1–2 stem sections per species, previously used for conductivity measurements) were embedded in paraffin, cut with a rotary microtome (Leica RM2245; Leica Biosystems) at 20 µm, and cross sections were stained with Safranin and AstraBlue (1% and 0.5% in distilled water, respectively) following standard protocols (Von Arx et al., 2016). Permanently fixed slides were scanned at ×10 magnification with a slide scanner (Axio Scan.Z1, Carl Zeiss Microscopy GmbH) and images were exported as JPGs.

2.6 | Detailed analyses for *A. uva-ursi*

Additional analyses were conducted for *A. uva-ursi* to better understand the development and characteristics of nonconductive conduits. This species was selected, as nonfunctionality was clearly related to xylem age, dysfunctions were reversible by high-pressure flushing, and stems were long enough for measurements in the centrifuge.

2.6.1 | Vitality staining

Short stem segments ($n = 3$) were treated with 0.5% (w/v) 2,3,5-Triphenyl-tetrazolium chloride (TTC; Larcher et al., 1969; Sturite et al., 2005) to test whether parenchyma cells in inner, non-conductive, growth rings were still living or dead, as the latter is the hallmark of heartwood formation in trees. TTC stains vital, metabolically active cells bright red due to a reduction of the compound to water insoluble formazan, while all other cells remain unstained. Therefore, stem segments of about 15 mm length were immersed for 48 h at room temperature in the TTC solution, then transferred to water, and within the following day cross sections from the middle part of each sample were analysed with a light microscope.

2.6.2 | Age-related changes in functionality

For several samples with varying stem diameter ($n = 15$), the number of total growth rings, the number of functional growth rings (all rings with >50% xylem area stained), the conductive and the total xylem area, as well as the conductivity were determined as described above. The number and percentage of functional annual rings, the absolute and percent conductive xylem area, as well as k_{sc} were related to the total number of growth rings.

2.6.3 | Vulnerability to cavitation

To test whether the conductivity pattern in *A. uva-ursi* was related to a higher xylem vulnerability to drought-induced embolism in older growth rings compared with recent rings, 25 cm long shoots ($n = 6$) were flushed repeatedly with distilled, filtered, and degassed water at 70 kPa to fill all conduits. Then the first part of the segment (length 15 cm) was cut off and debarked, and negative Ψ from −0.5 to −1.5 MPa were induced in the sample by use of centrifugal force (Alder et al., 1997). Therefore, branches were fixed in a 150-mm rotor in a Sorvall RC-5 centrifuge (Thermo Fisher Scientific) and spinning velocity necessary to impose the desired water potential at the segment's centre was applied following the protocol given in Beikircher et al. (2010). After spinning, segments were re-cut under water to obtain 4- to 6-cm-long stem segments from the samples' centre. Perfusion with safranin was conducted for this stressed segment as well as of the control section (distal part of the flushed shoot not used for centrifugation) and for both the staining pattern and the stained area were determined on cross sections from the segment centre as described before.

2.7 | Statistics

All values are given as mean ± *SE*. Differences between species and between k_s and k_{sc} were analysed with the Bonferroni test (for data with homogeneity of variance, tested with the Levene test) or

Tamhane test (no homogeneity of variance) after testing for Gaussian distribution with the Kolmogorov–Smirnov test. Regressions were calculated by dynamic fitting based on polynomial linear and quadratic equations. For each plot, the fitted regression model with the higher coefficient of determination was visualized with the 95% confidence interval. All tests (two-tailed) were performed pairwise at a probability level of 5% using SPSS (version 24; SPSS) and SigmaPlot (version 13; Systat Software Inc.).

3 | RESULTS

3.1 | Functionality of conduits

Both safranin staining and micro-CT measurements showed nonconducting conduits under saturated conditions in all analysed dwarf shrubs (Figure 1). The combined results of both methods revealed that these conduits were air-filled and partly regained the capacity to conduct water following high-pressure flushing (Table 2). However, the proportion and distribution of nonfunctional elements within stems largely varied among species, while results were consistent within species and across study sites (see also Figure S3). In the following, the distribution, proportion, and reversibility of hydraulic dysfunctions of plants at the main study area near Innsbruck are presented:

3.1.1 | Distribution of nonfunctional conduits

Three distinct patterns of dysfunctional areas in the several-year-old (>4 years) stems were identified. Three dwarf shrub species (*V. myrtillus*, *V. gaultherioides*, and *C. vulgaris*) exhibited a ring of nonconductive conduits within each annual increment (Figure 1; see also 3D reconstruction in Figure S6). Although recognition of growth ring borders in these shrubs is challenging, nonfunctional conduits were observed to be located predominantly in the latewood, whereby the transition from water to gas-filled xylem areas was either sharply delineated (e.g., *V. gaultherioides*) or rather smooth (e.g., *C. vulgaris*; Figure 1). In contrast, in the two species *A. uva-ursi* and *K. procumbens* the older growth rings were not conductive at all, while younger rings remained completely functional. For the latter species, the micro-CT scan even indicated that only the current-year ring was conductive. Finally, *E. carnea* exhibited a scattered occurrence of embolised conduit groups within the stem. CT scans of the same samples with fully embolised xylem (following cutting and dehydration) and a microscopic image of wood cross sections are reported in Supplemental Figure S2 and S5 for better recognition of the overall occurrence of conduits in the wood of analysed species.

3.1.2 | Proportion of nonfunctional conduits

Quantification was based on samples stained by safranin, as limited access time to the synchrotron facility restrained the number of micro-CT scans per species. The proportion of nonconductive xylem area in the stem cross section varied between 19.26% and 49.52% (Table 2). While *E. carnea* with an irregular occurrence of air-filled conduits had the lowest value, the highest proportion of nonconductive elements was detected for *A. uva-ursi* (Figure 2a).

3.1.3 | Reversibility of hydraulic dysfunctions

In part of the species, nonfunctional conduits were completely blocked and not removable by high-pressure flushing (*V. myrtillus*, *V. gaultherioides*, *E. carnea*), in others they were partially (*C. vulgaris*, *K. procumbens*) or completely (*A. uva-ursi*) conductive following flushing (Table 2). Reversibility was thus not linked to a specific cross-sectional pattern of dysfunction.

3.2 | Specific hydraulic conductivity

The specific hydraulic conductivity (k_s) varied significantly between the species and ranged from 1.38×10^{-4} m^2 s^{-1} MPa^{-1} in *V. gaultherioides* to 3.57×10^{-4} m^2 s^{-1} MPa^{-1} in *A. uva-ursi* (Table 2). As a consequence of nonconducting xylem areas and their varying proportion on the total xylem area, the corrected hydraulic conductivity (k_{sc}) significantly differed from k_s (except for *E. carnea*) and was considerably higher in all species (Figure 2b).

Plant k_{sc} was closely related to $xylem_{cond}$ (Figure 3), whereby species with low $xylem_{cond}$ had high k_{sc}. Only *E. carnea* had a comparably high k_{sc} and high $xylem_{cond}$.

3.3 | Detailed analysis of *A. uva-ursi*

The additional analyses on *A. uva-ursi* revealed that the parenchyma of inner, hydraulically nonfunctional xylem parts was still metabolically active, as shown by the TTC-staining (Figure S4). Parenchyma cells in all growth rings were stained with no differences between older and more recent rings.

The extent of conducting xylem was closely related to stem age, whereby the number of active xylem rings increased with age while their overall percentage decreased (Figure 4). Furthermore, $xylem_{cond}$, whose calculation is based on area measurements, decreased significantly with plant age. In addition, k_{sc} was positively correlated with cambial age, indicating that younger (=outer) growth rings exhibited a higher specific conductivity than older ones.

The exposure of flushed branches to xylem tension in the centrifuge experiment showed a clear pattern of appearing dysfunctions in the stressed shoots. Inner (older) annual rings embolised already at −0.5 to −1.5 MPa, while younger growth rings at these tensions were still conductive (Figure 5).

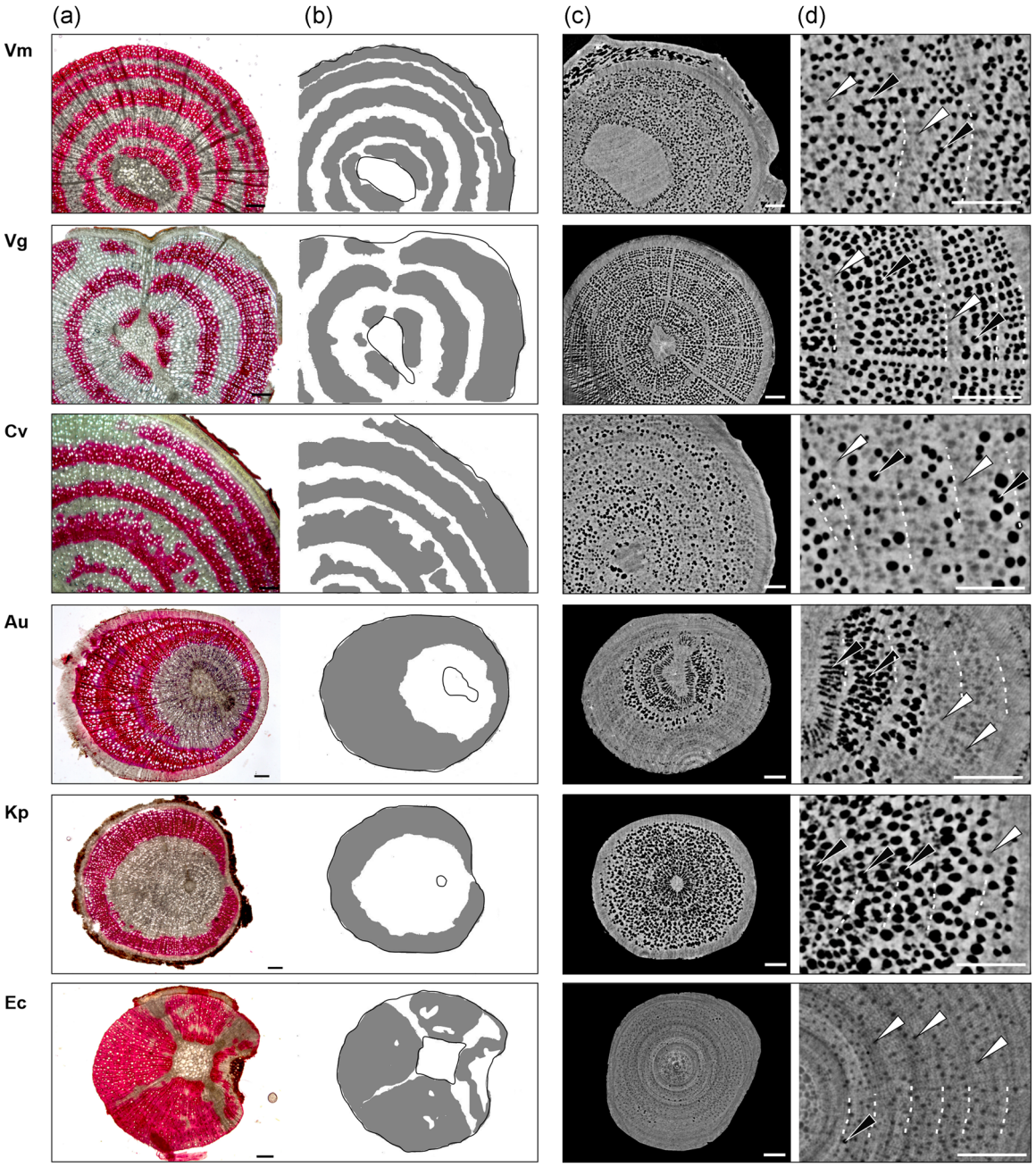

FIGURE 1 Safranin staining and micro-computed tomography (micro-CT) scans visualizing the distribution of functionally active and nonactive conduits in the stem cross section of saturated plants. By perfusion with safranin (a) conducting elements appear red, while the rest of the xylem area remains unstained. Subsequent image analysis (b) enabled to determine the conducting (depicted in grey) and nonfunctional (depicted in white) xylem area. In reconstructed cross sections following micro-CT measurements (c,d), water-filled conduits appear light grey (white arrows) and air-filled elements appear dark grey (black arrows). White dashed lines indicate borders between annual rings. Due to the methodology, different samples for staining and CT scans had to be used. *Vaccinium myrtillus* (Vm), *V. gaultherioides* (Vg), *Calluna vulgaris* (Cv), *Arctostaphylosuva-ursi* (Au), *Kalmia procumbens* (Kp), and *Erica carnea* (Ec); scale bars = 200 μm

4 | DISCUSSION

This study provides detailed insight into occurrence and cross-sectional distribution of nonfunctional xylem conduits by noninvasive synchrotron-based micro-CT visualization, safranin staining, and flow measurements in a group of unstressed and fully hydrated plants during the growing season. The observations suggest that persistent nonconducting xylem elements are widespread in the dwarf shrub growth form and occur in regular, stable, and species-specific patterns including complete decommission of older growth rings, partial dysfunctions in each growth ring, and scattered occurrence of small inactive xylem areas. While the decommission of inner growth

TABLE 2 Percent of conducting xylem area ($xylem_{cond}$), specific hydraulic conductivity (k_s), corrected specific hydraulic conductivity (k_{sc}, related to the conducting xylem area), the reversibility of nonconducting conduits determined by safranin staining and repeated flushing at high pressure, and number of analysed samples (*n*) of *Vaccinium myrtillus* (Vm), *V. gaultherioides* (Vg), *Calluna vulgaris* (Cv), *Arctostaphylos uva-ursi* (Au), *Kalmia procumbens* (Kp), and *Erica carnea* (Ec)

	$Xylem_{cond}$ (%)	k_s (m^2 s^{-1} MPa^{-1} $\times10^{-4}$)	k_{sc} (m^2 s^{-1} MPa^{-1} $\times10^{-4}$)	Reversible	*n*
Vm	67.19 ± 2.96^{bc}	2.21 ± 0.21^{b}	$3.22 \pm 0.23^{b*}$	No	10
Vg	67.47 ± 4.20^{bc}	1.38 ± 0.10^{a}	$2.16 \pm 0.11^{a*}$	No	10
Cv	62.88 ± 3.62^{ab}	3.00 ± 0.19^{bc}	$4.82 \pm 0.24^{c*}$	Partly	10
Au	50.48 ± 7.21^{a}	3.57 ± 0.67^{c}	$8.19 \pm 1.50^{d*}$	Yes	10
Kp	65.47 ± 5.49^{bc}	2.51 ± 0.30^{b}	$3.79 \pm 0.23^{bc*}$	Partly	10
Ec	80.74 ± 5.64^{c}	2.57 ± 0.37^{b}	3.41 ± 0.35^{bc}	No	10

Note: Mean ± *SE*. Significant differences between the species are indicated by different letters and between k_s and k_{sc} by asterisks.

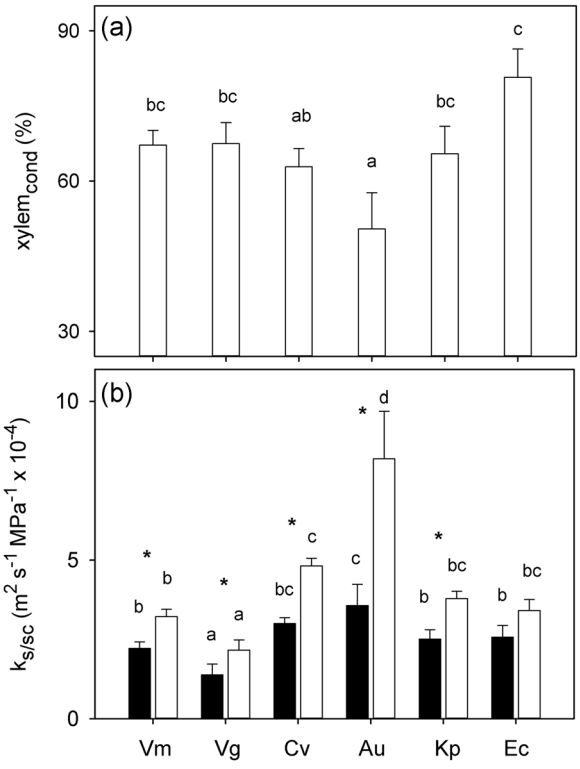

FIGURE 2 (a) Percent of conducting xylem area ($xylem_{cond}$) and (b) specific hydraulic conductivity (k_s; black bars) and corrected specific hydraulic conductivity (k_{sc}, related to the conducting xylem area; white bars) of *Vaccinium myrtillus* (Vm), *V. gaultherioides* (Vg), *Calluna vulgaris* (Cv), *Arctostaphylos uva-ursi* (Au), *Kalmia procumbens* (Kp), and *Erica carnea* (Ec). Mean ± *SE*, significant differences between the species are indicated by different letters, and between k_s and k_{sc} by asterisks

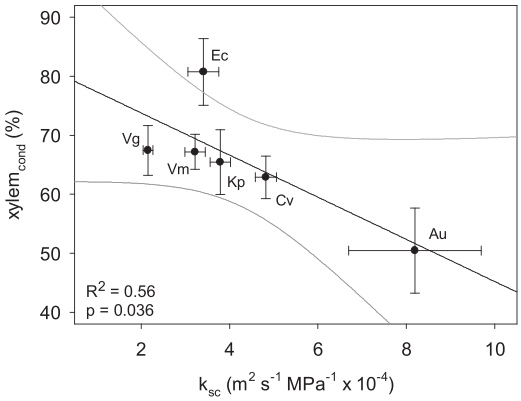

FIGURE 3 Relation between percent conducting xylem area ($xylem_{cond}$) and corrected specific hydraulic conductivity (k_{sc}). Symbols represent mean ± *SE* for each species. *Vaccinium myrtillus* (Vm), *V. gaultherioides* (Vg), *Calluna vulgaris* (Cv), *Arctostaphylos uva-ursi* (Au), *Kalmia procumbens* (Kp), and *Erica carnea* (Ec)

rings was clearly related to stem age and a higher vulnerability to cavitation of older rings, no satisfying functional explanation for the high proportion of nonfunctional conduits in each annual ring could be detected. However, across species and dysfunctional patterns, lower xylem fractions contributing to the transport function were balanced by a higher hydraulic efficiency of the conducting areas. Depending on the species, nonconductive conduits were permanently blocked (probably by gums and tyloses; De Micco et al., 2016) or air bubbles blocked the water flow but were removable by high pressure flushing. Permanent occlusions were not visible in our microCT scans, probably because their visualization is difficult, particularly for gums, and requires specific image processing (compare Maranon-Jiminez et al., 2017).

4.1 | Dysfunction patterns

The large inter-specific differences in xylem functionality could not be related to the phylogenetic classification of analysed shrubs (compare Kron et al., 2002). For example, the species *C. vulgaris*, *E. carnea*, *K. procumbens* all belong to the clade Ericoideae but showed strongly divergent distribution patterns of nonfunctional conduits and varying dysfunction reversibility (see Figure 1 and Table 2). The complexity of cross-sectional dysfunction patterns may, though, reflect varying plant adaptations to water availability and diverse carbon and wood space allocation strategies (Bittencourt et al., 2016). Dwarf shrub species with dysfunctions in each annual ring grow on more humid sites than species with dysfunction in older rings and form belowground runners instead of creeping shoots (Table 1). Hydraulic patterns thus could also have implications on the viability and competitiveness of individual species under changing environmental conditions, with large impacts on plant community composition, structure, and function.

Basically, hydraulic dysfunctions in a certain proportion of the stem can be based on variations in (a) the xylem resistance to

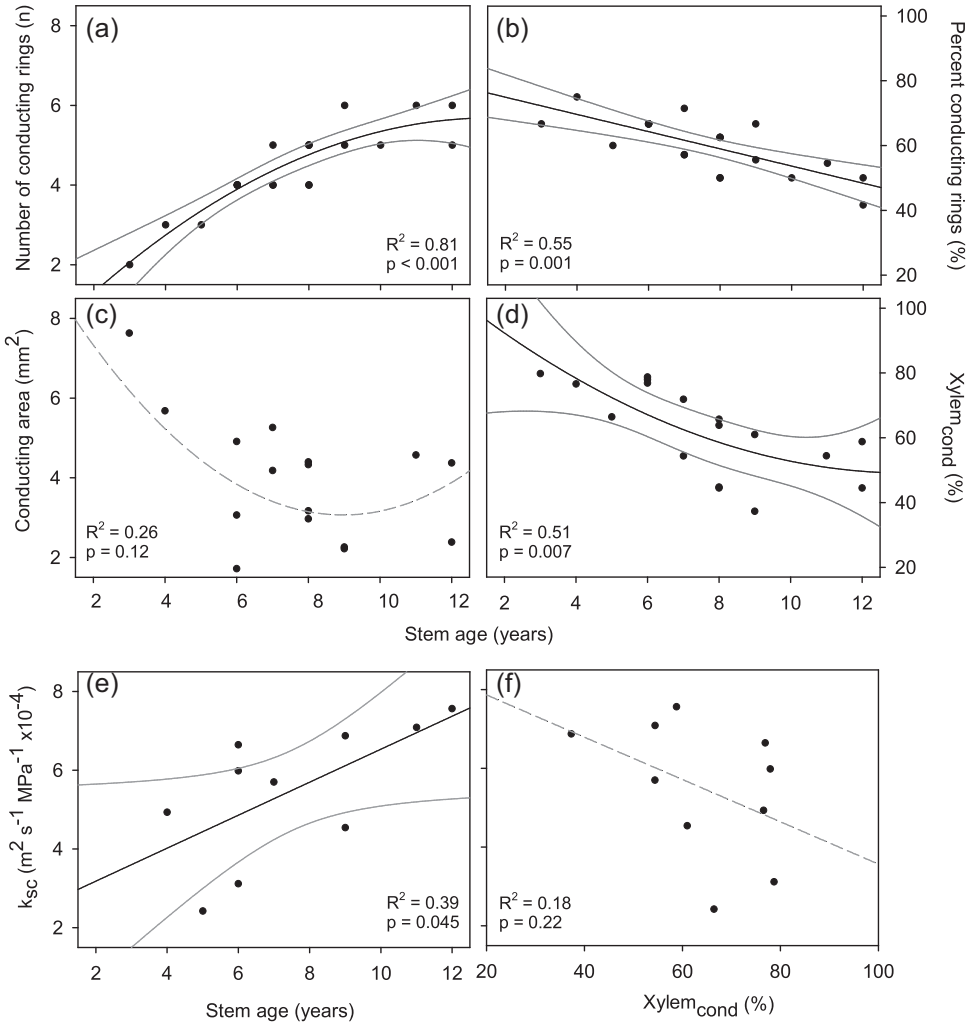

FIGURE 4 Relation of (a) number of conducting annual rings, (b) percent conducting annual rings, (c) conducting xylem area, and (d) percent conducting xylem area ($xylem_{cond}$) with the number of total rings (corresponding to stem age) in *Arctostaphylos uva-ursi*. In addition, relation of the corrected specific hydraulic conductivity (k_{sc}) with (e) stem age and (f) $xylem_{cond}$. Shown are the regression lines with 95% confidence intervals

cavitation, and/or (b) the capacity to repair embolised conduits. Cavitation events in Alpine dwarf shrubs are unlikely to be caused by summer drought stress, as several studies indicate a rather unproblematic water regime in these plant communities during summer (Anadon-Rosell et al., 2017; Ganthaler & Mayr, 2021). During winter, in contrast, freeze-thaw events are frequent and winter drought (in case of lacking snow protection) may be intense (Grabherr, 1980; Sperry & Sullivan, 1992). Such freeze-thaw induced cavitation was shown to appear mainly in winter or early spring and can be either refilled during the next season (Utsumi et al., 1998; Zhang et al., 2018) or, particularly in the case of ring-porous species, remain nonfunctional (Utsumi et al., 1996). Yet, different patterns of xylem dysfunctions in studied dwarf shrubs may have different causes and consequences.

The restriction of water transport to recent growth rings (in this study demonstrated for *A. uva-ursi* and *K. procumbens*; Figure 1) is known to occur in many woody plants (Hölttä et al., 2013; Tyree & Zimmermann, 2002). When the stem gets progressively larger in diameter, older xylem tissues loose hydraulic functionality (see also Section 1). The detailed analyses on *A. uva-ursi* revealed, that the number of conductive growth rings is constantly increasing until the plants are a few years old but then this increase levels off; their share on the total number of rings as well as $xylem_{cond}$ are thus overall decreasing (Figure 4). Simultaneously increasing k_{sc} with plant age will anyhow ensure adjusted conductance to increasing leaf area and plant height (Petit & Anfodillo, 2009). Higher vulnerability of inner annual rings, as repeatedly reported (e.g., Fukuda et al., 2015; Melcher et al., 2003) and shown here for *A. uva-ursi* (Figure 5), points to cavitation fatigue (Hacke et al., 2001) as an important cause for dysfunction of older xylem areas. They probably withstand some but not too many cycles of cavitation and refilling (compare results for diffuse-porous trees in Utsumi et al., 1998). A metabolically active parenchyma, which is an important prerequisite for potential embolism refilling, (Secchi et al., 2017) was found even in dysfunctional

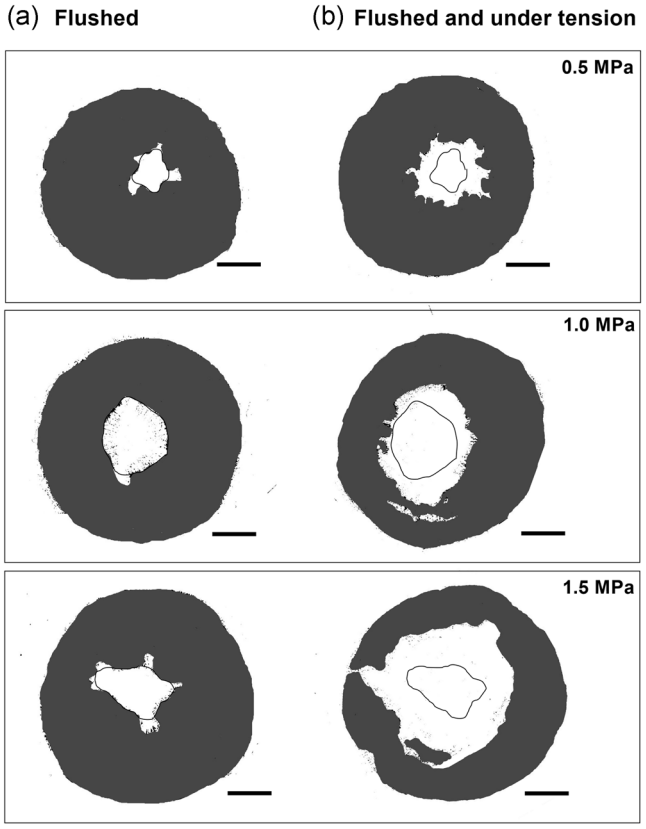

FIGURE 5 Enhanced vulnerability to cavitation in older growth rings of *Arctostaphylos uva-ursi*. If saturated branch samples were first flushed at high pressure to fill most conduits (a) and then exposed to tension of 0.5–1.5 MPa in the centrifuge (b), embolism formation was firstly detected in the inner growth rings. Visualized by staining with safranin; cross-sectional xylem areas recognized as conductive are shown in grey (for details see Section 2), scale bars = 100 μm

areas (Figure S4). Remarkably, living parenchyma and the (mostly) absence of permanent conduit occlusions (Table 2) in inner growth rings is contrary to heartwood characteristics in trees.

In contrast, nonconductive vessels and tracheids in each growth ring (here detected for *V. myrtillus*, *V. gaultherioides* and *C. vulgaris*; Figure 1) evidence varying functional lifespans (and potentially different functionalities) of xylem elements formed during the year and must be differentiated clearly from changes during plant aging. There are several observations that vessels can undergo development, gain and loss of hydraulic functionality within a single growing season (Jacobsen et al., 2018; Tyree & Zimmermann, 2002). This applies to earlywood vessels in various ring- or semi-ring-porous temperate tree species (e.g., oaks, ashes, elms, and chestnuts; Kitin & Funada, 2016) which tend to cavitate earlier than latewood vessels due to their larger diameter and related pit characteristics, consequently leading to a large proportion of inactive xylem at the end of the season (e.g., Dai et al., 2020; Jacobsen et al., 2007, 2015; Sperry & Sullivan, 1992). Regular and persistent dysfunctions in the latewood of each annual ring, like found in analysed dwarf shrubs, are scarcely known (Jacobsen et al., 2018; Umebayashi et al., 2010) and do not seem to be related to conduit diameter (compare also Figures S2 and S5). Jacobsen et al. (2018) reported them for some arid and semi-arid shrub species, while Umebayashi et al. (2010) found them in diffuse-porous evergreen trees, among *Camellia sinensis* and *Vaccinium bracteatum*. Although vessel size seems not to be the main factor here, lower cavitation resistance and/or reduced repair capacity of the latewood may anyhow be based on structural differences, such as pit characteristics and connectivity between conduits and of conduits with adjacent living cells affecting embolism spread and refilling (Knipfer et al., 2015; Loepfe et al., 2007; Secchi et al., 2017), which needs further investigations. Interestingly, species with nonfunctional conduits in each annual ring in our study all show solitary vessels, while species with dysfunctions in older rings have grouped vessels (Table S1; Schweingruber & Landolt, 2005), indicating that conductive patterns may be related to xylem network topology (Loepfe et al., 2007; see also Schenk et al., 2008). A distinct vessel-free latewood zone can only be found in *A. uva-ursi* (Figure S5; Schweingruber et al., 2011) but not in the species with dysfunctions in each annual ring (Figures S2, S5 and S6). We also exclude that non-stained xylem areas contained developing conduits that were not yet hydraulically functional (compare Jacobsen et al., 2018), as they occurred in each annual ring.

In *E. carnea*, dysfunctional areas were distributed irregularly and across growth rings, so that early- and latewood of old and young growth rings were affected. The pattern indicates that embolism spread from the centre (air-filled pith) and single embolised vessels towards the periphery (Figure 1; for patterns of embolism spreading in trees see, for example, Guan et al., 2021; Mayr et al., 2006).

4.2 | Physiological implications

Varying functional lifespan of conduits can induce seasonal changes in hydraulic efficiency and safety, as in the growth phase functional xylem areas are increasing (through formation of new xylem), while they are decreasing in a cavitation phase (also reducing the proportion of hydraulically most vulnerable stem compartments; compare Dai et al., 2020; Klein et al., 2018; Zhang et al., 2018; and results for *V. myrtillus* in Ganthaler & Mayr, 2015a). Moreover, dysfunctions can act as a source for gas movement into adjacent sap-filled conduits in drought-stressed angiosperm xylem ('air-seeding'; Tyree & Zimmermann, 2002). A high proportion of nonconductive air-filled xylem elements may thus affect the hydraulic safety by enhancing embolism propagation (compare Guan et al., 2021; Mayr et al., 2006; Roth-Nebelsick, 2019), particularly if nonfunctional conduits appear in each annual ring and the connectivity of the xylem network is high (as indicated by grouped vessels; see also Loepfe et al., 2007). However, hydraulic integration and high redundancy in the xylem network in this context could also be beneficial by offering alternative transport routes (Ewers et al., 2007). Interestingly, for several desert shrubs species, a functional division and strong hydraulic segmentation of sapwood sectors was reported, leading to independent hydraulic units (Espino & Schenk, 2009; Schenk

et al., 2008). Poorly interconnected conduits across ring borders and between functional and nonfunctional compartments could prevent embolism spread also in the Alpine dwarf shrubs.

Probably the most important consequence of a reduced functional lifespan of conduits is the strongly decreased water transport efficiency of the plant stem (Table 2; Figure 2), even though k_{sc} in remaining functional xylem of analysed dwarf shrubs was comparable to branch k_s of subalpine trees (Mayr & Cochard, 2003). Higher k_{sc} of species with lower proportion of conductive xylem (Figure 3) also indicates compensation of lost transport capacities. Observed xylem dysfunctions may not be limiting for water relations of Alpine dwarf shrubs and comparably low conductivity could anyhow match water demand due to less acquisitive leaf traits and slower growth, as well as due to lower growth height compared with trees (Pratt & Jacobsen, 2017; Sanchez-Martinez et al., 2020). Based on shorter transport distances due to the shorter stature, a higher hydraulic resistance and thus steeper water potential gradients between roots and leaves are less relevant. Though it remains difficult to understand from an evolutionary and resource-use perspective why plants invest in xylem elements that lose their function within comparably short periods, particularly because knowledge of a potential post-hydraulic-function of these conduits is lacking. We hypothesize that nonfunctional xylem areas contribute to mechanical stability (mainly relevant for upright and not for creeping dwarf shrubs, compare Table 1), as similarly reported for highly vulnerable and inefficient compression wood (Mayr & Cochard, 2003). Lignified conduit walls make a considerable contribution to mechanical support (Crivellaro & Büntgen, 2020) and, due to their multi-cellular long structure, vessels may provide higher tensile strength than fibres (Wang et al., 2014). Besides, nonconductive xylem parts may serve as important nonstructural carbohydrate storage sites which are still connected to the phloem by living parenchyma cells (see Hartmann & Trumbore, 2016).

For trees, patterns and proportions of inactive xylem conduits were mainly analysed with regard to the formation of heartwood and radial patterns in sap flow (e.g., Jimenez et al., 2000; Nadezhdina et al., 2002), embolization in ring-porous species (Knipfer et al., 2019; Utsumi et al., 1996), embolism spread during desiccation (Gauthey et al., 2020; Hargrave et al., 1994; Lamarque et al., 2018) and annual cycles of winter cavitation and refilling (Utsumi et al., 1998). Systematic persistent dysfunctions in recent growth rings during the growing season received less attention, and seem to be highly variable (e.g., Jimenez et al., 2000). However, persistent dysfunctional xylem areas could be expected to have pronounced effects also on tree hydraulics (see e.g., Dai et al., 2020), as trees are exposed to higher hydraulic stress due to height and leaf area and are known to exhibit relatively small hydraulic safety margins (Choat et al., 2012; Gleason et al., 2016). Detailed analyses of consistent and regular xylem dysfunctions, their pattern and underlying structural–functional trade-offs in trees under natural operating range of xylem pressures) would thus help to get a more comprehensive understanding of plant hydraulic functioning.

4.3 | Methodical aspects

From a methodical point of view, it must be noted that a high proportion of nonfunctional xylem conduits, which are present in hydrated plants and in part are permanently blocked or simply air-filled, can complicate and adversely affect several classical hydraulic methods (compare Sergent et al., 2020). This especially applies if the presence and nature of dysfunctions is unknown and the error thus not assessed correctly. Dysfunctions reversible by high pressure flushing or vacuum infiltration (Table 2) lead to the perception of artificially high embolism rates in measurements according to the method of Sperry et al. (1988) and therefore wrong percent loss of conductivity values. Moreover, different levels of dysfunction might lead to different shapes of vulnerability curves and complex patterns of functional versus nonfunctional conduits may in some cases explain the highly discussed observation of sigmoidal and non-sigmoidal vulnerability curves (see Roth-Nebelsick, 2019). Perfusion of samples with dye in this context represents a good approach for rapid and immediate control measurements, while noninvasive micro-CT visualization, if available, is probably the best solution for detailed and comprehensive analyses. Both approaches can also substantially improve the interpretation of k_s values, especially if related to conduit traits such as vessel size and pit characteristics, and the calculation of the hydraulic conductance (see also Brodersen et al., 2019).

5 | CONCLUSIONS

Nonconductive xylem areas strongly affect the plant hydraulic efficiency and potentially also the hydraulic safety and should be analysed and considered more frequently in hydraulic studies and modelling approaches. The presented work indicates that persistent dysfunctions in hydrated plants are frequent for Alpine dwarf shrubs and shows that they can occur in complex, species-specific, and regular cross-sectional patterns. We thus recommend to (1) be careful when interpreting hydraulic measurements without knowledge of the conduit functionality and eventual reversibility of dysfunctions, and (2) use staining and noninvasive methods more frequently to visualize the xylem functionality in hydrated and unstressed plants. Results indicate a functional interrelation between the specific hydraulic conductivity and the proportion of functional xylem, but underlying trade-offs between hydraulic efficiency and safety, mechanical support, and conduit investment require further investigations, including various growth forms and plants growing under divergent environmental conditions.

ACKNOWLEDGEMENTS

The study was supported by the L'Oreal Austria fellowship 'For Women in Science' and a researcher excellence grant (Austrian Federal Ministry for science and research) to AG and the Austrian Science Fund (FWF) project P29896, P32203, I4918, and J4300 and conducted within the frame of the research area 'Alpiner Raum' of the University of Innsbruck. Access to the SYRMEP beamline was

granted and funded by Elettra-Sincrotone Trieste (proposal 20165277).

CONFLICT OF INTERESTS

The authors declare that there are no conflict of interests.

DATA AVAILABILITY STATEMENT

All main results are presented within the manuscript and the supplementary materials. The raw data that support the findings of this study are available from the corresponding author upon reasonable request.

ORCID

Andrea Ganthaler http://orcid.org/0000-0002-8670-6199
Andreas Bär http://orcid.org/0000-0002-0059-3964
Adriano Losso http://orcid.org/0000-0001-7839-4941
Andrea Nardini http://orcid.org/0000-0002-5208-0087
Christian Dullin http://orcid.org/0000-0003-4297-8077
Georg von Arx http://orcid.org/0000-0002-8566-4599
Stefan Mayr http://orcid.org/0000-0002-3319-4396

REFERENCES

Alder, N.N., Pockman, W.T., Sperry, J.S. & Nuismer, S. (1997) Use of centrifugal force in the study of xylem cavitation. *Journal of Experimental Botany*, 48(3), 665–674.

Anadon-Rosell, A., Hasibeder, R., Palacio, S., Mayr, S., Ingrisch, J., Ninot, J.M. et al. (2017) Short-term carbon allocation dynamics in subalpine dwarf shrubs and their responses to experimental summer drought. *Environmental and Experimental Botany*, 141, 92–102.

Beikircher, B., Ameglio, T., Cochard, H. & Mayr, S. (2010) Limitation of the Cavitron technique by conifer pit aspiration. *Journal of Experimental Botany*, 61(12), 3382–3393.

Beikircher, B. & Mayr, S. (2016) Avoidance of harvesting and sampling artefacts in hydraulic analyses: a protocol tested on *Malus domestica*. *Tree Physiology*, 36(6), 797–803.

Bittencourt, P.R.L., Pereira, L. & Oliveira, R.S. (2016) On xylem hydraulic efficiencies, wood space-use and the safety-efficiency tradeoff. *New Phytologist*, 211(4), 1152–1155.

Brodersen, C.R., Roddy, A.B., Wason, J.W. & McElrone, A.J. (2019) Functional status of xylem through time. *Annual Review of Plant Biology*, 70, 407–433.

Brun, F., Pacilè, S., Accardo, A., Kourousias, G., Dreossi, D., Mancini, L. et al. (2015) Enhanced and flexible software tools for x-ray computed tomography at the Italian Synchrotron Radiation Facility Elettra. *Fundamenta Informaticae*, 141(2–3), 233–243.

Carrer, M., Pellizzari, E., Prendin, A.L., Pividori, M. & Brunetti, M. (2019) Winter precipitation - not summer temperature—is still the main driver for Alpine shrub growth. *Science of the Total Environment*, 682, 171–179.

Cernusca, A. (1976) Energie- und Wasserhaushalt eines alpinen Zwergstrauchbestandes während einer Föhnperiode. *Archives for Meteorology, Geophysics, and Bioclimatology, Series B*, 24, 219–241.

Choat, B., Jansen, S., Brodribb, T.J., Cochard, H., Delzon, S., Bhaskar, R. et al. (2012) Global convergence in the vulnerability of forests to drought. *Nature*, 491(7426), 752–756.

Choat, B., Brodersen, C.R. & McElrone, A.J. (2015) Synchrotron X-ray microtomography of xylem embolism in *Sequoia sempervirens* saplings during cycles of drought and recovery. *New Phytologist*, 205(3), 1095–1105.

Choat, B. & Pittermann, J. (2009) New insights into bordered pit structure and cavitation resistance in angiosperms and conifers. *New Phytologist*, 182(3), 557–560.

Cochard, H., Delzon, S. & Badel, E. (2015) X-ray microtomography (micro-CT): a reference technology for high-resolution quantification of xylem embolism in trees. *Plant, Cell and Environment*, 38(1), 201–206.

Crivellaro, A. & Büntgen, U. (2020) New evidence of thermally constrained plant cell wall lignification. *Trends in Plant Science*, 25(4), 322–324.

Dai, Y., Wang, L. & Wan, X. (2020) Frost fatigue and its spring recovery of xylem conduits in ring-porous, diffuse-porous, and coniferous species in situ. *Plant Physiology and Biochemistry*, 146, 177–186.

De Micco, V., Balzano, A. & Wheeler, E.A. (2016) Tyloses and gums: a review of structure, function and occurrence of vessel occlusions. *IAWA Journal*, 37(2), 186–205.

Espino, S. & Schenk, H.J. (2009) Hydraulically integrated or modular? Comparing whole-plant-level hydraulic systems between two desert shrub species with different growth forms. *New Phytologist*, 183(1), 142–152.

Ewers, F.W., Ewers, J.M., Jacobsen, A.L. & López-Portillo, J. (2007) Vessel redundancy: modeling safety in numbers. *IAWA Journal*, 28(4), 373–388.

Fukuda, K., Kawaguchi, D., Aihara, T., Ogasa, M.Y., Miki, N.H., Haishi, T. et al. (2015) Vulnerability to cavitation differs between current-year and older xylem: non-destructive observation with a compact magnetic resonance imaging system of two deciduous diffuse-porous species. *Plant, Cell and Environment*, 38(12), 2508–2518.

Ganthaler, A. & Mayr, S. (2015a) Dwarf shrub hydraulics: two *Vaccinium* species (*V. myrtillus*, *V. vitis-idaea*) of the European Alps compared. *Physiologia Plantarum*, 155(4), 424–434.

Ganthaler, A. & Mayr, S. (2015b) *Vaccinium gaultherioides*: another insight into water relations of alpine dwarf shrubs. *Journal of Plant Hydraulics*, 2, e-004.

Ganthaler, A. & Mayr, S. (2021) Subalpine dwarf shrubs differ in vulnerability to xylem cavitation: an innovative staining approach enables new insights. *Physiologia Plantarum*, 172, 2011–2021. Available from: https://doi.org/10.1111/ppl.13429

Gärtner, H., Lucchinetti, S. & Schweingruber, F.H. (2014) New perspectives for wood anatomical analysis in dendrosciences: the GSL1-microtome. *Dendrochronologia*, 32(1), 47–51.

Gauthey, A., Peters, J.M.R., Carins-Murphy, M.R., Rodriguez-Dominguez, C.M., Li, X., Delzon, S. et al. (2020) Visual and hydraulic techniques produce similar estimates of cavitation resistance in woody species. *New Phytologist*, 228(3), 884–897.

Gleason, S.M., Westoby, M., Jansen, S., Choat, B., Hacke, U.G., Pratt, R.B. et al. (2016) Weak tradeoff between xylem safety and xylem-specific hydraulic efficiency across the world's woody plant species. *New Phytologist*, 209(1), 123–136.

Grabherr, G. (1980) Variability and ecology of the alpine dwarf shrub community Loiseleurio-Cetrarietum. *Vegetatio*, 41(2), 111–120.

Guan, X., Pereira, L., McAdam, S., Cao, K.F. & Jansen, S. (2021) No gas source, no problem: Proximity to pre-existing embolism and segmentation affect embolism spreading in angiosperm xylem by gas diffusion. *Plant, Cell and Environment*, 44, 1329–1345. Available from: https://doi.org/10.1111/pce.14016

Hacke, U., Stiller, V., Sperry, J.S., Pittermann, J. & McCulloh, K.A. (2001) Cavitation fatigue. Embolism and refilling cycles can weaken the cavitation resistance of xylem. *Plant Physiology*, 125(2), 779–786.

Hargrave, K.R., Kolb, K.J., Ewers, F.W. & Davis, S.D. (1994) Conduit diameter and drought induced embolism in *Salvia mellifera* Greene (Labiatae). *New Phytologist*, 126(4), 695–705.

Hartmann, H. & Trumbore, S. (2016) Understanding the roles of non-structural carbohydrates in forest trees - From what we can measure to what we want to know. *New Phytologist*, 211(2), 386–403.

Hietz, P., Rosner, S., Sorz, J. & Mayr, S. (2008) Comparison of methods to quantify loss of hydraulic conductivity in Norway spruce. *Annals of Forest Science*, 65(5), 502.

Hölttä, T., Kurppa, M. & Nikinmaa, E. (2013) Scaling of xylem and phloem transport capacity and resource usage with tree size. *Frontiers in Plant Science*, 4, 496.

Hubbard, R.M., Stiller, V., Ryan, M.G. & Sperry, J.S. (2001) Stomatal conductance and photosynthesis vary linearly with plant hydraulic conductance in ponderosa pine. *Plant, Cell and Environment*, 24(1), 113–121.

Jacobsen, A.L., Pratt, R.B., Davis, S.D. & Ewers, F.W. (2007) Cavitation resistance and seasonal hydraulics differ among three arid Californian plant communities. *Plant, Cell and Environment*, 30(12), 1599–1609.

Jacobsen, A.L., Rodriguez-Zaccaro, F.D., Lee, T.F., Valdovinos, J., Toschi, H.S., Martinez, J.A. et al. (2015) Grapevine xylem development, architecture and function. In: Hacke, U.G. (Ed.) *Functional and ecological xylem anatomy*. Cham: Springer. pp. 133–162.

Jacobsen, A.L., Valdovinos-Ayala, J. & Pratt, R.B. (2018) Functional lifespans of xylem vessels: Development, hydraulic function, and post-function of vessels in several species of woody plants. *American Journal of Botany*, 105(2), 142–150.

Jimenez, S.M., Nadezhdina, N., Cermak, J. & Morales, D. (2000) Radial variation in sap flow in five laurel forest tree species in Tenerife, Canary Islands. *Tree Physiology*, 20(17), 1149–1156.

Kitin, P. & Funada, R. (2016) Earlywood vessels in ring-porous trees become functional for water transport after bud burst and before the maturation of the current-year leaves. *IAWA Journal*, 37(2), 315–331.

Klein, T., Zeppel, M.J.B., Anderegg, W.R.L., Bloemen, J., De Kauwe, M.G., Hudson, P. et al. (2018) Xylem embolism refilling and resilience against drought-induced mortality in woody plants: processes and trade-offs. *Ecological Research*, 33(5), 839–855.

Knipfer, T., Brodersen, C.R., Zedan, A., Kluepfel, D.A. & McElrone, A.J. (2015) Patterns of drought-induced embolism formation and spread in living walnut saplings visualized using X-ray microtomography. *Tree Physiology*, 35(7), 744–755.

Knipfer, T., Reyes, C., Earles, J.M., Berry, Z.C., Johnson, D., Brodersen, C.R. et al. (2019) Spatiotemporal coupling of vessel cavitation and discharge of stored xylem water in a tree sapling. *Plant Physiology*, 179(4), 1658–1668.

Körner, C. (2003) *Alpine plant life. Functional plant ecology of high mountain ecosystems*, 2nd edn. Berlin: Springer.

Kron, K.A., Judd, W.S., Stevens, P.F., Crayn, D.M., Anderberg, A.A., Gadek, P.A. et al. (2002) Phylogenetic classification of Ericaceae: Molecular and morphological evidence. *Botanical Review*, 68(3), 335–423.

Lamarque, L.J., Corso, D., Torres-Ruiz, J.M., Badel, E., Brodribb, T.J., Burlett, R. et al. (2018) An inconvenient truth about xylem resistance to embolism in the model species for refilling *Laurus nobilis* L. *Annals of Forest Science*, 75, 88.

Landolt, E. (2010) *Flora indicativa. Ökologische Zeigerwerte und biologische Kennzeichen zur Flora der Schweiz und der Alpen*, 2nd edition. Bern: Haupt Verlag.

Larcher, W., Bauer, H., Bendetta, G., Harrasser, J., Hilscher, H. & Mair, B. (1969) Anwendung und Zuverlässigkeit der Tetrazoliummethode zur Feststellung von Schäden in pflanzlichen Geweben. *Mikroskopie*, 25, 207–218.

Larcher, W. (2003) *Physiological plant ecology: Ecophysiology and stress* physiology of functional groups, 4th edition. Berlin Heidelberg New York: Springer.

Loepfe, L., Martinez-Vilalta, J., Pinol, J. & Mencuccini, M. (2007) The relevance of xylem network structure for plant hydraulic efficiency and safety. *Journal of Theoretical Biology*, 247(4), 788–803.

Losso, A., Bär, A., Dämon, B., Dullin, C., Ganthaler, A., Petruzzellis, F. et al. (2019) Insights from in vivo micro-CT analysis: testing the hydraulic vulnerability segmentation in *Fagus sylvatica* and *Acer pseudoplatanus* seedlings. *New Phytologist*, 221(4), 1831–1842.

Maestre, F.T., Eldridge, D.J. & Soliveres, S. (2016) A multifaceted view on the impacts of shrub encroachment. *Applied Vegetation Science*, 19(3), 369–370.

Maranon-Jiminez, S., Van den Bulcke, J., Piayda, A., Van Acker, J., Cuntz, M., Rebmann, C. et al. (2017) X-ray computed microtomography characterizes the wound effect that causes sap flow underestimation by thermal dissipation sensors. *Tree Physiology*, 38(2), 288–302.

Mayr, S. & Cochard, H. (2003) A new method for vulnerability analysis of small xylem areas reveals that compression wood of Norway spruce has lower hydraulic safety than opposite wood. *Plant, Cell and Environment*, 26(8), 1365–1371.

Mayr, S., Rothart, B. & Wolfschwenger, M. (2006) Temporal and spatial pattern of embolism induced by pressure collar techniques in twigs of *Picea abies*. *Journal of Experimental Botany*, 57(12), 3157–3163.

Mayr, S., Schmid, P., Beikircher, B., Feng, F. & Badel, E. (2020) Die hard: timberline conifers survive annual winter embolism. *New Phytologist*, 226(1), 13–20.

Melcher, P.J., Zwieniecki, M.A. & Holbrook, N.M. (2003) Vulnerability of xylem vessels to cavitation in sugar maple. Scaling from individual vessels to whole branches. *Plant Physiology*, 131(4), 1775–1780.

McCulloh, K.A. & Woodruff, D.R. (2012) Linking stomatal sensitivity and whole-tree hydraulic architecture. *Tree Physiology*, 32(4), 369–372.

McDowell, N., Barnard, H., Bond, B., Hinckley, T., Hubbard, R., Ishii, H. et al. (2002) The relationship between tree height and leaf area: sapwood area ratio. *Oecologia*, 132(1), 12–20.

Nadezhdina, N., Čermák, J. & Ceulemans, R. (2002) Radial patterns of sap flow in woody stems of dominant and understory species: scaling errors associated with positioning of sensors. *Tree Physiology*, 22(13), 907–918.

Nardini, A., Savi, T., Losso, A., Petit, G., Pacilè, S., Tromba, G. et al. (2017) X-ray microtomography observations of xylem embolism in stems of *Laurus nobilis* are consistent with hydraulic measurements of percentage loss of conductance. *New Phytologist*, 213(3), 1068–1075.

Neuner, G. (2014) Frost resistance in alpine woody plants. *Frontiers in Plant Science*, 5, 654.

Nolf, M., Rosani, A., Ganthaler, A., Beikircher, B. & Mayr, S. (2016) Herb hydraulics: Inter- and intraspecific variation in three *Ranunculus* species. *Plant Physiology*, 170(4), 2085–2094.

Paganin, D., Mayo, S.C., Gureyev, T.E., Miller, P.R. & Wilkins, S.W. (2002) Simultaneous phase and amplitude extraction from a single defocused image of a homogeneous object. *Journal of Microscopy*, 206(1), 33–40.

Petit, G. & Anfodillo, T. (2009) Plant physiology in theory and practice: Analysis is of the WBE model for vascular plants. *Journal of Theoretical Biology*, 259(1), 1–4.

Petruzzellis, F., Pagliarani, C., Savi, T., Losso, A., Cavalletto, S., Tromba, G. et al. (2018) The pitfalls of in vivo imaging techniques: evidence for cellular damage caused by synchrotron X-ray computed micro-tomography. *New Phytologist*, 220(1), 104–110.

Pratt, R.B. & Jacobsen, A.L. (2017) Conflicting demands on angiosperm xylem: tradeoffs among storage, transport and biomechanics. *Plant, Cell and Environment*, 40(6), 897–913.

Roth-Nebelsick, A. (2019) It's contagious: calculation and analysis of xylem vulnerability to embolism by a mechanistic approach based on epidemic modelling. *Trees*, 33(5), 1519–1533.

Sanchez-Martinez, P., Martinez-Vilalta, J., Dexter, K.G., Segovia, R.A. & Mencuccini, M. (2020) Adaptation and coordinated evolution of plant hydraulic traits. *Ecology Letters*, 23(11), 1599–1610.

Schenk, H.J., Espino, S., Goedhart, C.M., Nordenstahl, M., Martinez-Cabrera, H.I. & Jones, C.S. (2008) Hydraulic integration and shrub growth form linked across continental aridity gradients. *Proceedings of the National Academy of Sciences of the United States of America*, 105(32), 11248–11253.

Schweingruber, F.H., Börner, A. & Schulze, E.D. (2011) *Atlas of stem anatomy in herbs, shrubs and trees*. Berlin: Springer.

Schweingruber, F.H. & Landolt, W. (2005) *The xylem database*. A web production of the Swiss Federal Research Institute WSL. Available at: https://www.wsl.ch/dendroprot/xylemdb [Accessed 19th November 2020].

Secchi, F., Pagliarani, C. & Zwieniecki, M.A. (2017) The functional role of xylem parenchyma cells and aquaporins during recovery from severe water stress. *Plant, Cell and Environment*, 40(6), 858–871.

Sergent, A.S., Varela, S.A., Barigah, T.S., Badel, E., Cochard, H., Dalla-Salda, G. et al. (2020) A comparison of five methods to assess embolism resistance in trees. *Forest Ecology and Management*, 468(15), 118175.

Sperry, J.S. (2003) Evolution of water transport and xylem structure. *International Journal of Plant Sciences*, 164(S3), 115–127.

Sperry, J.S. (2013) Cutting-edge research or cutting-edge artefact? An overdue control experiment complicates the xylem refilling story. *Plant, Cell and Environment*, 36(11), 1916–1918.

Sperry, J.S., Donnelly, J.R. & Tyree, M.T. (1988) A method for measuring hydraulic conductivity and embolism in xylem. *Plant, Cell and Environment*, 11(1), 35–40.

Sperry, J.S. & Sullivan, J.E.M. (1992) Xylem embolism in response to freeze-thaw cycles and water stress in ring-porous, diffuse-porous, and conifer species. *Plant Physiology*, 100(2), 605–613.

Sturite, I., Henriksen, T.M. & Breland, T.A. (2005) Distinguishing between metabolically active and inactive roots by combined staining with 2, 3,5-triphenyltetrazolium chloride and image colour analysis. *Plant and Soil*, 271(1), 75–82.

Taneda, H. & Sperry, J.S. (2008) A case-study of water transport in co-occurring ring- versus diffuse-porous trees: contrasts in water-status, conducting capacity, cavitation and vessel refilling. *Tree Physiology*, 28(11), 1641–1651.

Tyree, M.T. & Zimmermann, M.H. (2002) *Xylem structure and the ascent of sap*. Berlin: Springer.

Umebayashi, T., Utsumi, Y., Koga, S., Inoue, S., Matsumura, J., Oda, K. et al. (2010) Xylem water-conducting patterns of 34 broadleaved evergreen trees in southern Japan. *Trees*, 24(3), 571–583.

Utsumi, Y., Sano, Y., Ohtani, J. & Fujikawa, S. (1996) Seasonal changes in the distribution of water in the outer growth rings of *Fraxinus mandshurica* var *japonica*: a study by cryo-scanning electron microscopy. *IAWA Journal*, 17(2), 113–124.

Utsumi, Y., Sano, Y., Fujikawa, S., Funada, R. & Ohtani, J. (1998) Visualization of cavitated vessels in winter and refilled vessels in spring in diffuse-porous trees by cryo-scanning electron microscopy. *Plant Physiology*, 117(4), 1463–1471.

Von Arx, G., Crivellaro, A., Prendin, A.L., Cufar, K. & Carrer, M. (2016) Quantitative wood anatomy—practical guidelines. *Frontiers in Plant Science*, 7, 781.

Wang, N., Liu, W., Huang, J. & Ma, K. (2014) The structure-mechanical relationship of palm vascular tissue. *Journal of the Mechanical Behavior of Biomedical Materials*, 36, 1–11.

Zhang, W., Feng, F. & Tyree, M.T. (2018) Seasonality of cavitation and frost fatigue in Acer mono Maxim. *Plant, Cell & Environment*, 41(6), 1278–1286.

SUPPORTING INFORMATION

Additional supporting information may be found in the online version of the article at the publisher's website.

How to cite this article: Ganthaler, A., Bär, A., Dämon, B., Losso, A., Nardini, A., Dullin, C. et al. (2022). Alpine dwarf shrubs show high proportions of nonfunctional xylem: Visualization and quantification of species-specific patterns. *Plant, Cell & Environment*, 45, 55–68. https://doi.org/10.1111/pce.14226